Astron. Astrophys. 304, 168–175 (1995)

ASTRONOMY AND ASTROPHYSICS

Astrometry of minor planets with Hipparcos

D. Hestroffer [1], **B. Morando** [1], **F. Mignard** [2], **and A. Bec-Borsenberger** [1]

[1] Bureau des Longitudes, URA CNRS 707, 77 av. Denfert Rochereau, F-75014 Paris, France
[2] Observatoire de la Côte d'Azur, Dept. CERGA, URA CNRS 1360, Av. N. Copernic, F-06130 Grasse, France

Received 29 November 1994 / Accepted 3 September 1995

Abstract. After the processing of 30 months of the observations carried out by Hipparcos it is possible to provide a reliable idea of the astrometric results to be obtained on the 48 minor planets included in the observing programme. Hipparcos observations are one-dimensional measurements of the separation of objects along a precessing scanning circle, these scanning circles are averaged over approximately 0.3 day yielding a reference great circle. The main output will consist of about 100 astrometric abscissae on a reference great circle for each minor planet with an individual accuracy of about 0.02arcsec. We discuss in this paper the reduction procedure and assess the systematic errors due to the shape and scattering properties of the asteroids. The use of the results to improve the orbital parameters of the minor planets as well as the link of the kinematical and dynamical frames is briefly touched upon in the last section.

Key words: astrometry – minor planets – methods: data analysis

1. Introduction

Observed asteroids, with well determined orbits permitting their recovery practically at each opposition, amount to nearly 4000 and their number increases regularly over the years. However the actual number for sizes greater than 1 km is thought to be one order of magnitude larger and currently more than 10000 asteroids have been found. While the members of the main belt are located between the orbits of Mars and Jupiter, there are families of earth-approaching objects on high elliptical orbits, usually not yet catalogued. Of the estimated 1000 earth-grazing asteroids over 1 km of diameter, less than 10 % have been catalogued so far. With the exception of the brightest members of the family, the minor planets are small objects, typically between 10 and 100 km in diameter, so that their angular diameter from the Earth is less than 0.1 arcsec. Some objects reach 0.2 arcsec and the largest, Ceres, with a diameter close to 950 km is observed by Hipparcos at a distance from the earth between 2 to 3.4 AU, corresponding respectively to angular diameters $0''63$ and $0''37$.

Send offprint requests to: D. Hestroffer

Sixty-three such minor planets brighter than magnitude 13 were proposed in the list of objects to be observed by the ESA satellite Hipparcos at an early level of the mission definition (Bec-Borsenberger, 1985). Eventually the final selection based on the observability ended up with 48 asteroids included in the final programme (Bec-Borsenberger, 1989) which were subsequently regularly observed during the 37 months of the mission. Ephemerides were computed every year and uplinked by ESOC along with the star coordinates to steer the observing programme.

The scientific objectives of the observations of the minor planets are at least twofold:

- To provide an indirect link between the dynamical reference frame used in the theory of their motion and the stellar kinematical frame represented by the Hipparcos catalogue, once it has been tied to the extragalactic frame (Söderhjelm and Lindegren, 1982, Bec-Borsenberger et al., 1995). This will be achieved thanks to the astrometric positions of the minor planets reduced in parallel with the stars in the Hipparcos reference system. It is expected that the plane of the ecliptic will be determined with respect to the Hipparcos catalogue to about 0.001 arcsec with a degradation of about 0.0007 arsec/year.
- To study the photometric signal which carries a wealth of information on the minor planets themselves. In particular the analysis of the modulation coefficients may constrain the scattering properties of the surface while the varying magnitude reduced to one astronomical unit gives indication on the rotation period and the shape of the asteroids, whatever their angular size.

2. Minor planets data

Basically the raw data provided by Hipparcos for a minor planet are very similar to those of a faint star. It differs essentially in two ways

- All the objects with a sizeable angular size, typically larger than 0.1 arcsec, yield a signal less modulated than the corresponding signal of a single star.
- The minor planets have a large daily motion, typically of 500 arcsec. However the data reduction scheme was de-

signed for the stars, in such a way that a geometric position is determined every half day. This is clearly not possible for the minor planets and implies that normal points should be produced over much shorter intervals.

2.1. The Hipparcos observations of minor planets

During the transit of a minor planet on the Hipparcos grid, one fits the observed count rate $S(t_k)$ for the k-th sample to a five parameter model defined by

$$S(t_k) = I + B + IM\cos(\omega t_k + \phi) + IN\cos(2\omega t_k + \psi) \qquad (1)$$

where I is the total intensity, B the unmodulated background, M and N the modulation coefficients of the first and second harmonic respectively and ϕ and ψ the corresponding phases. For a pointlike object we have typically $M = M_0 = 0.72$ and $N = N_0 = 0.25$ and $\psi \approx 2\phi$. However as soon as the angular size of the source is larger than 0.1 arcsec the modulation gets smaller. The effect has been studied in detail in several papers (Morando, 1985, 1987, Morando and Lindegren, 1989). The main conclusion of these works is the fact that both the amplitudes and the phases of the signal depend as much on the minor planet diameter as on its surface scattering properties or albedo distribution. At present, it is not possible to discriminate among these factors from the analysis of the modulation curves. To get a good order of magnitude, one can use the approximation of an uniformly illuminated spherical source of apparent diameter ρ with the phase angle i (the angular distance between the sun and the earth as seen from the minor planet) equal to zero. In such a case the modulation coefficients are given by $M/M_0 = 2\,J_1(\pi\,\rho/s)/(\pi\,\rho/s)$ and $N/N_0 = 2\,J_1(2\,\pi\,\rho/s)/(2\,\pi\,\rho/s)$, where $J_1(x)$ is the Bessel function of order 1 and s is the Hipparcos gridstep, $s = 1.208$ arcsec. Up to and including Ceres, one can expand these expressions to the fourth order with a sufficient accuracy by

$$M/M_0 = 1 - \frac{\pi^2}{8}\frac{\rho^2}{s^2} + \frac{\pi^4}{192}\frac{\rho^4}{s^4}$$

$$N/N_0 = 1 - \frac{\pi^2}{2}\frac{\rho^2}{s^2} + \frac{\pi^4}{12}\frac{\rho^4}{s^4}$$

For a source with a centre of symmetry and zero phase angle there is no phase shift between the two harmonics and the phase of the first harmonic is tied to the position of the geometric centre of the minor planet. This important property does no longer hold when the phase angle reaches values as large as 20 deg as shown in Morando and Lindegren (1989). The most worrying problem is the displacement of the photocentre from the centre of figure of the minor planet, which may be much larger than the expected measurement error for the largest minor planets. In the following astrometric reduction no attempt is made so far to correct for this effect, as it depends too much on the scattering model. So the results for normal places pertain only to the small asteroids with angular diameter less than 0.1 arcsec, when the uncertainty on the position due to scattering and shape effect is at most 0.003 arcsec; this is the case for 25 minor planets. Except for asteroids 1-Ceres, 2-Pallas, 4-Vesta and 10-Hygiea, with angular diameter greater than 0.2 arcsec, this uncertainty is however lower than the precision of the reduced astrometric position (see Sect. 5.1).

2.2. The data organization

The catalogue of positions used in this work is that of the FAST consortium, first intermediate 30-month solution. It is issued after 30 months of observations and is built from an iterated 18-month solution where the remaining 12 months were added with no further iteration (Kovalevsky et al., 1995).

The minor planets retained for the mission are listed in Table 1. The third column contains the observed magnitude averaged over the 30 months of observations. The angular diameter expressed in arcseconds, is given for a spherical object at quadrature assuming a circular orbit. The fifth column corresponds to the number of reference great circles where the minor planet was observed. The last column gives the number of transits during the 30-month mission and after rejection of suspicious data (see Sect. 4.2.1).

The data compression between the photon counts and the parameters of the modulated signal is carried out during the Hipparcos mass treatment, with no distinction whatsoever on the structure of the object observed: either a single or multiple star, or a minor planet or one of the satellites of Jupiter and Saturn included in the programme. An overview of the methods used is given in Kovalevsky et al. (1992) and Donati et al. (1992). The difference appears in the determination of the abscissa on the reference great circle. This intermediate reduction step concludes with a geometric abscissa of a star about every 12 hours, corrected for the light aberration due to the motion of the earth and that of the satellite and for the relativistic light deflection. This position is determined by fitting an observation model to about 30 to 40 grid abscissae collected over these 12 hours. The basic assumption made is that over an interval of few hours, the change in the geometric coordinates of a star can be linearized.

As said before this assumption fails for the minor planets because of their fast orbital motion. So the output of the circle reduction consists of about 30 to 40 abscissae corresponding to the apparent positions of the minor planets projected on the reference circle. By apparent it is meant that the aberration, both due to the satellite and minor planet motion, has not been removed from the abscissae. These observations are delivered in chronological order, and sorted by asteroid for each reference circle. Each circle is defined in a specific file by the coordinates of its pole while the origins of the abscissae are supplied by the Hipparcos sphere solution and made available to the minor planet data processing. The photometric solution is read in parallel in order to identify grid crossings polluted by the light of a bright star that happens to be in the neighborhood of the minor planet, either in the same field of view or in the complementary field. Such an occurrence may affect a few percent of the transits, which ultimately are to be rejected.

Table 1. List of minor planets included in the Hipparcos programme along with the basic statistics of the observation. The angular diameter is given at quadrature and is expressed in arcsec

IAU No.	Name	Mean magnitude	Angular diameter	Num. of circles	Num. of transits
1	Ceres	8.5	0.49	14	48
2	Pallas	9.5	0.28	12	36
3	Juno	11	0.14	18	58
4	Vesta	8	0.32	15	52
5	Astraea	11.5	0.07	23	76
6	Hebe	10.5	0.12	19	87
7	Iris	10	0.13	17	59
8	Flora	11	0.10	14	46
9	Metis	10.5	0.11	13	42
10	Hygiea	11.5	0.20	14	42
11	Parthenope	11.5	0.10	22	65
12	Victoria	11.5	0.08	5	14
13	Egeria	12	0.12	11	36
14	Irene	11.5	0.09	12	44
15	Eunomia	10.5	0.15	17	70
16	Psyche	11.5	0.13	14	48
18	Melpomene	11.5	0.10	20	91
19	Fortuna	12	0.14	9	26
20	Massalia	11	0.10	13	47
22	Kalliope	12	0.09	18	54
23	Thalia	12	0.06	13	49
27	Euterpe	11	0.07	9	33
28	Bellona	12	0.07	3	12
29	Amphitrite	10.5	0.13	18	60
30	Urania	12	0.06	15	47
31	Euphrosyne	12	0.11	5	15
37	Fides	11.5	0.06	8	31
39	Laetitia	11.5	0.08	27	108
40	Harmonia	12	0.08	17	59
42	Isys	11	0.07	15	52
44	Nysa	11.5	0.05	11	39
51	Nemausa	12	0.10	5	13
63	Ausonia	12	0.07	3	8
88	Thisbe	12	0.11	10	37
115	Thyra	12	0.05	6	18
129	Antigone	12	0.06	11	41
192	Nausikaa	11.5	0.07	6	19
196	Philomela	12	0.07	5	16
216	Kleopatra	12	0.07	6	20
230	Athamantis	12	0.07	12	31
324	Bamberga	11.5	0.13	18	73
349	Dembowska	11.5	0.07	24	99
354	Eleonora	11.5	0.09	18	70
451	Patientia	12	0.11	8	27
471	Papagena	11.5	0.07	25	109
511	Davida	12	0.15	13	46
532	Herculina	11	0.12	12	36
704	Interamnia	11.5	0.16	19	73
Total					2282

Because of the particular directions of the satellite spin axis, minor planets and satellites observations only occur near quadrature. The apparent position on the reference circle is given for every frame (approximately 2.13 sec) for one crossing. The minor planet observation data consist in pairs of preceding and following transits spread around quadrature, each transit containing typically 8 great circle abscissae and the corresponding errors (rms).

3. The a priori Ephemerides

The computed position of each minor planet is determined by numerical integration from the set of its ecliptical osculating elements (Bulirsh and Stoer, 1966; Balmino, 1969). The coordinates of the disturbing planets are calculated by use of the DE 200 ephemerides (Standish, 1990). These elements, first taken from "Ephemerides of minor planets", published by the Institute of Theoretical Astronomy in Leningrad (1966), have been improved so that the observed positions differ by less than 1 arcsecond from the calculated positions. For this improvement, the observations published by the Minor Planet Center (Cincinatti), have been used in addition to those made during a special campaign of observations, started in 1983, by the European observatories of Bordeaux, La Palma, San Fernando and Fabra, i.e. more than 15000 observations, in the framework of the preparation of the Hipparcos mission (Bec-Borsenberger, 1992). The last set of orbital elements computed by Bec-Borsenberger (1993) is used as initial conditions, at the epoch JED 2447800.5 (October 1, 1989 at 0 hours), close to the beginning of the observations of Hipparcos.

4. Data processing for the astrometry of minor planets

4.1. Reduction to great circle abscissae

For comparison to the apparent observed direction, the calculated astrometric position is corrected for the satellite parallax and aberration and the gravitational deflection of light by the sun. To these, the photocentre displacement due to phase effect can be added. From the satellite tracking one knows its geocentric position and velocity vector. From this, and from the velocity of the earth relative to the solar system barycentre, we correct the observations for the parallactic effect due to our observing from a moving platform at a distance up to 42000 km from the earth's centre. The precision of this correction is that of the ephemeris, that is to say about 1000 km (0.5 arcsec at 2.5 au) , or $3\text{x}10^{-6}$ in relative precision. The error in the correction is then less than 0.1 mas, well below the quality of the observations.

Then comes the correction for aberration which is computed to the second order in v/c. With $\boldsymbol{v}$ the barycentric satellite velocity and $\boldsymbol{u}$ the minor planet direction with respect to the satellite, the correction is:

$$d\boldsymbol{u} = (1 + \frac{1}{2c}\,\boldsymbol{u}\cdot\boldsymbol{v})\,\frac{\boldsymbol{v}}{c}$$

and the apparent direction is given by $\boldsymbol{u} + d\boldsymbol{u}$.

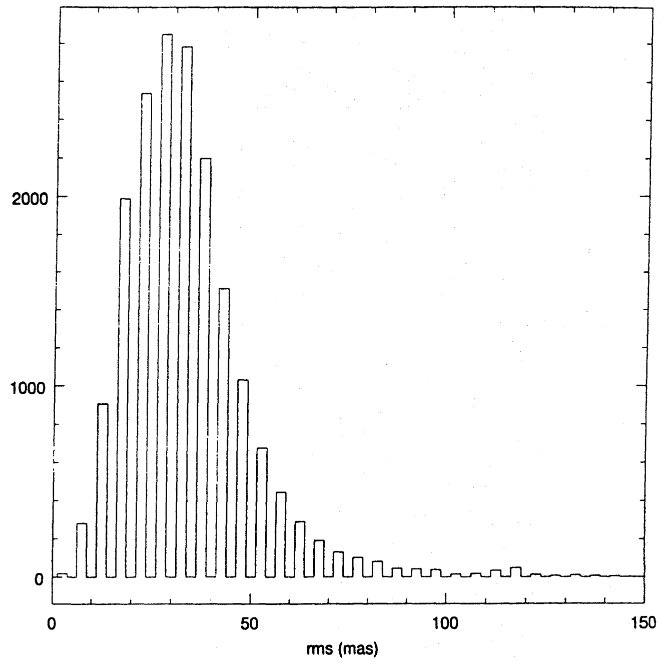

Fig. 1. Distribution of the precision of the observations at the frame level

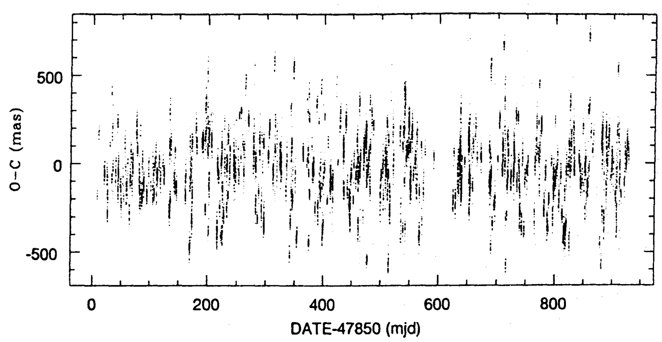

Fig. 2. Observed minus computed abscissae for the whole dataset

As for the light ray deflection, it must be computed by taking into account the fact that unlike the stars, the source lies at a relatively close distance. From the general derivation given by Will (1981), the angular correction to the object elongation ψ is obtained as:

$$\Delta\psi = \frac{2m_\odot}{a}\,\frac{r_o}{\Delta}\,\frac{1+\cos(\psi+i)}{\sin\psi} \quad ; \quad \frac{2m_\odot}{a} = 4.07\ mas$$

where i is the phase angle, r_o, Δ are respectively the object heliocentric and geocentric distances. Finally the computed abscissae are obtained by projection on the reference circle.

4.2. Analysis of the residuals

4.2.1. Computation of the residuals

This computation is made for observations with given rms lower than 0.1 arcsec only since, for the limiting magnitude of Hipparcos observations, positions with greater rms can be considered suspicious. For each frame k of a minor planet transit we can now compute the difference $(o-c)_k$ between the apparent observed and calculated abscissa on the reference circle. At this stage grid step ambiguities may still affect the observed position and cannot be detected systematically because of too low a precision in both the minor planet predicted position and the ephemeris uplinked by ESOC (these ephemerides are deduced from numerical integration and compressed into Chebyshev polynomials). However a grid step correction is systematically applied for each residual whose modulus is greater than 0.81 arcsec.

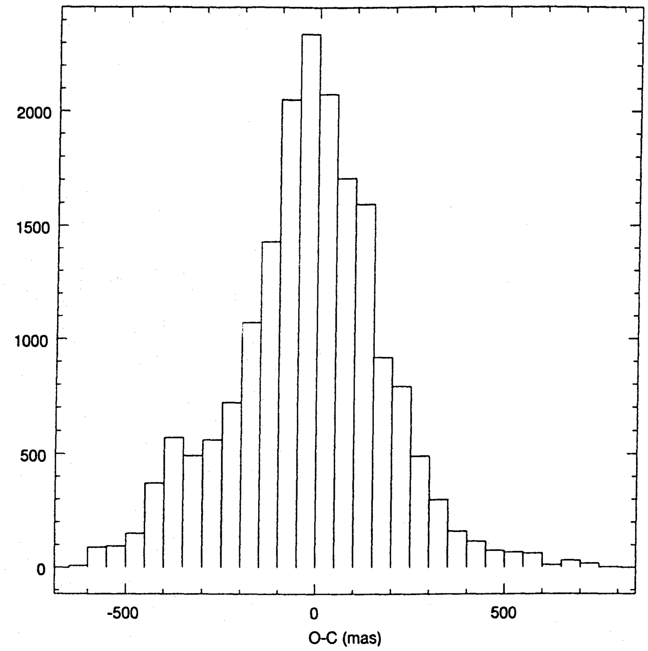

Fig. 3. Distribution of the O-C's for the whole data set

A minor planet crosses one of the telescope fields in approximately 18 s. Over this duration the projected velocity on the reference circle can be considered as well known so that the slopes of the observed and calculated places should be identical. Transits which do not satisfy this condition should be recognized and possibly removed. Let λ_k^o be the observed apparent abscissa for frame k at time t_k with root mean square σ_k, we can write:

$$\begin{cases} \lambda_k^o = a^o + b(t_k - t_0) + r_k \quad ; \quad r_k \text{being the true error} \\ \lambda_k^c = a^c + b(t_k - t_0) \end{cases}$$

The differences $\lambda_k^o - \lambda_k^c$ should not show any time trend but only an offset. Let $\overline{a_o}$ be the weighted mean of $\lambda_k^o - \lambda_k^c$ and $v_k = \lambda_k^o - \lambda_k^c - \overline{a_o}$ the corresponding residuals. We can reject suspicious transits after applying a χ^2 test on the estimated mean error per unit weight $\tilde{\sigma}_o$ of the residuals v_k. We have:

$$\tilde{\sigma}_o^2 = \frac{\sum p_k^2 v_k^2}{N-1} \quad ; \quad p_k = \frac{\sigma_o}{\sigma_k}$$

or, introducing the weighted mean $\overline{(o-c)}$ of the $(o-c)_k$

$$\tilde{\sigma}_o^2 = \frac{\sum p_k^2\,[(o-c)_k - \overline{(o-c)}]^2}{N-1}$$

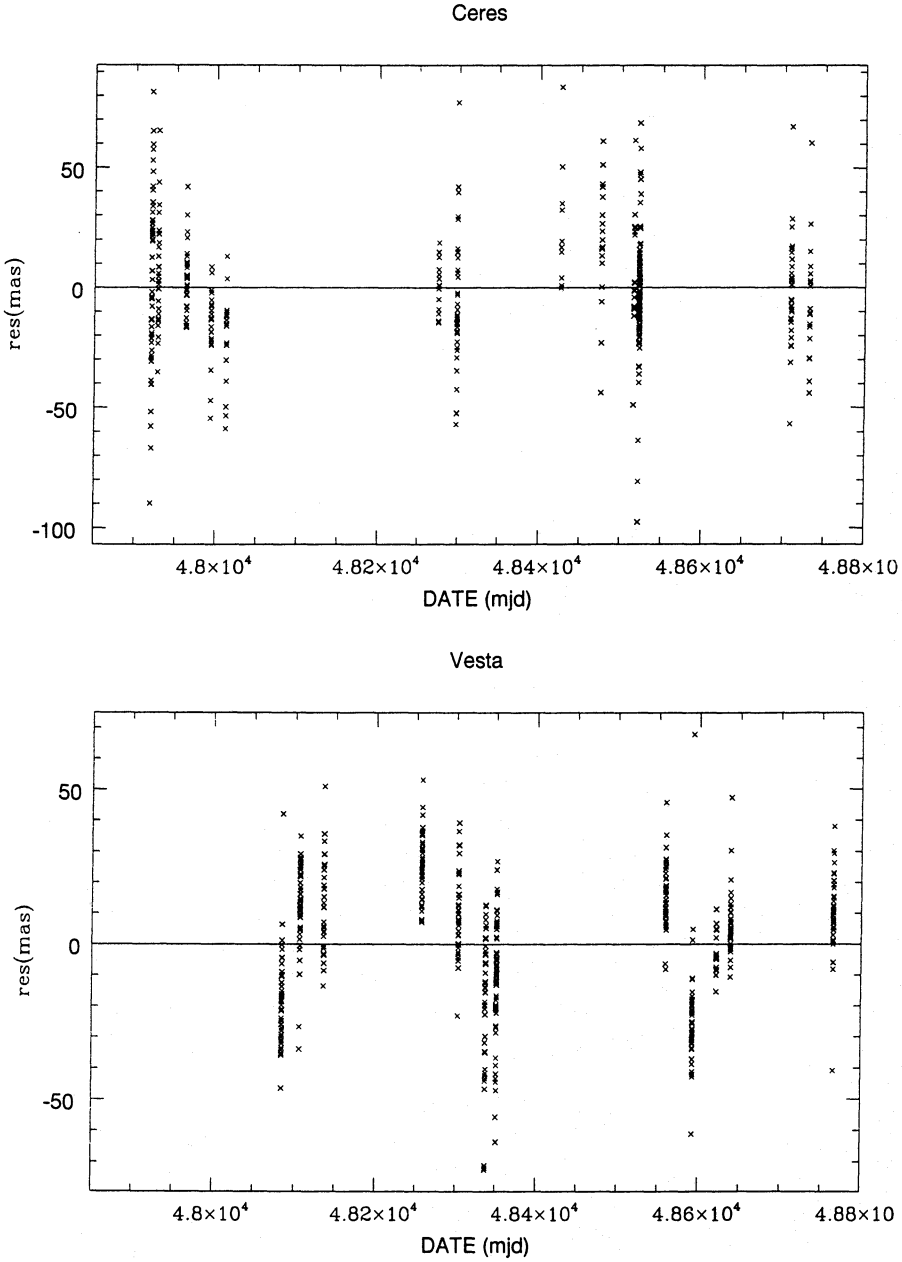

Fig. 4. Residuals for 1-Ceres and 4-Vesta

requiring the only evaluation of quantities $(o-c)_k$.

Typically we have $N = 8$. From rejection criteria at the 1% level it follows that, with $\sigma_o = 0.03$ arcsec, transits with $\tilde{\sigma}_o > 0.05$ arcsec are removed.

4.2.2. Discussion

Residuals were constructed for the 30 months data. Rejected observations with given rms greater than 0.1 arcsecond represent 1.6% of the raw data and the rejection of suspicious transits affects 1.9% of it. Fig. 1 shows a histogramme of the precision of the observations at the frame level. This precision depends on the minor planet magnitude and apparent diameter, the greater the magnitude or the apparent diameter is, the lower is the signal to noise ratio; at the frame level this precision is of the order of 0.03 arcsec. The o-c's on the different RGCs and with no phase effect correction are given as a function of time in Fig. 2; apart from the grid step ambiguity, these o-c's essentially reflect the minor planets ephemerides errors and vary from -0.6 to 0.8 arcsecond. For one minor planet, residuals are clustered over one or successive reference great circles, or on a time span of the order of one day; over this time the scatter is essentially due to the measurement noise. The scatter between different days present in Fig. 2 arises from the fact that: the reference circle oscillates around an instantaneous plane perpendicular to the ecliptic, yielding thus a periodical variation of the sign of these o-c's; and also because the entire dataset for all the asteroids is considered. As shown in the histogramme in Fig. 3 these ephemerides agree with the observations within a range of 0.5 arcsecond.

5. Further use of the results

5.1. Unidimensional positional astrometry

The apparent observed positions are reduced to an astrometric unidimensional position on a reference circle. The satellite parallax correction (up to 20 arcseconds) as well as the gravitational light deflection (lower than 0.01 arcsecond) depend on the minor planet's distance; but for the sub milli-arcsecond precision involved here the computed distance obtained from direct numerical integration is sufficient as shown earlier. For each transit we construct a normal point: mean abscissa at mid-transit time t_0. As said before at this time scale the observed $\tilde{\lambda}^o$ and calculated $\tilde{\lambda}^c$ astrometric abscissae slopes can be considered identical ($\tilde{b}^o = \tilde{b}^c = \tilde{b}$). The mean transit abscissa is then estimated by the median of the slope-reduced positions:

$$< \tilde{\lambda} >= med\{\tilde{\lambda}^o_k - \tilde{b}(t_k - t_0)\}$$

which is robust against outliers.

$$\sigma^2(< \tilde{\lambda} >) \simeq \frac{\pi}{2}\frac{1}{N}\frac{\sum(\lambda^o_k - \tilde{b}(t_k - t_0) - < \tilde{\lambda} >)^2}{N-1}$$

The latter estimation of deviation yields to a precision of typically 0.015 arcsecond for the transit normal abscissa.

5.2. Improvement of the orbital elements

The differences between the apparent observed places and the corresponding computed ones based on the best available ephemeris are typically 100 to 200 mas. These deviations are larger than the random error on the observations. So we can use the Hipparcos observations to determine new initial conditions, or equivalently to fit improved orbital elements. The variations of initial conditions are expressed in terms of a 6 parameters vector $\boldsymbol{dq} = (dl_o; dp; dq; dr; de; da/a)$ which is related to the osculating elements (Brouwer & Clemence, 1961). The approximation of the partial derivatives matrix B' (given in their set III) assuming a Keplerian orbit is still sufficient here so that we can write:

$$(o-c) = \frac{\boldsymbol{z} \wedge \boldsymbol{u}}{(\boldsymbol{z} \wedge \boldsymbol{u})^2} . \boldsymbol{du} = \frac{\boldsymbol{z} \wedge \boldsymbol{u}}{(\boldsymbol{z} \wedge \boldsymbol{u})^2} . B' . \boldsymbol{dq} = B . \boldsymbol{dq} \qquad (1)$$

where $\boldsymbol{z}$ is the reference circle pole direction and $\boldsymbol{u}$ is the minor planet position with respect to Hipparcos. A solution for the variation $\boldsymbol{dq}$ is then found by the least squares method. Table 2 gives, for some minor planets, the corrections to the initial osculating elements as well as the estimated errors. One sees that the orientation of the corrected orbit can be found with very great precision: dp and dq, which are directly related to the inclination and the longitude of the node, are accurate up to the mas level. This means that they are explicitely determined from the Hipparcos observations (not strongly correlated) and also found with a great precision. Thus the plane of the ecliptic is better fixed than the position of the dynamical equinox. The correlation between the other parameters $(dl_o; dr; de; da/a)$ arises from too short an observation time span as opposed to the minor planet sidereal periods, and from the particular geometry of observations (a scanning circle oscillates around a plane perpendicular to the ecliptic). Then least square estimates are known to be larger than the true value; so singular value decomposition (SVD) was used to find a better set of parameters to be determined. The solution of system (1) is neither unique (the normal matrix is "quasi rank deficient") nor does it minimize the square of the residuals. The correction is the particular SVD solution with minimal modulus that keeps the residuals in agreement (in the sense of the variance ratio F-test) with the one obtained by a standard solution. The magnitude of the correction determined here is of the order of 1 to 100 milli-arcsec. For about ten minor planets, up to four or five independent parameters can be estimated. Some of these minor planets are listed on Table 2 as well as the rank dimension retained. The set of new osculating elements that we obtain in this way is just one particular solution of the solutions fitting the Hipparcos observations over 30 months; when combined with the eigenvectors corresponding to the adopted null space of the normal matrix, it could yield an additional constraint to the fits to all existing classical observations available.

5.3. Photocentre displacement

The cases of Ceres and Vesta are of particular interest because, as shown in Fig. 4 the residuals, based on the new orbits, show systematic effects. For these minor planets the phase effect (opposite in magnitude to the measurement noise) should not be neglected even for the improvement of the minor planet orbital elements. At quadrature, the magnitude of this effect – depending essentially on the minor planet radius and the light scattering – will range between 5 and 25 mas for Ceres and between 3 and 15 mas for Vesta. For a spherical object with homogeneous surface and a scattering law following the reciprocity principle, the displacement is deduced by projection on the sky of vector $\boldsymbol{dp}$ along the phase angle bissector $\boldsymbol{x}$ and proportional to the object radius R: $\boldsymbol{dp} = R . C(i).\boldsymbol{x}$ (Lindegren, 1977). When considering a theoretical uniform brightness we find:

$$\boldsymbol{dp} = R . (C_u(i).\boldsymbol{x} + \alpha.\boldsymbol{u}) \quad ; \quad C_u(i) = \frac{8}{3\pi} . \sin i/2$$

where α is of no interest here. In addition, for $0.25\,rad < i < 0.5\,rad$, the expression of $C(i)$ can be linearized (Lindegren, 1987). The observed direction is then deduced from the position $\boldsymbol{u}$, with respect to Hipparcos, of the centre of mass by:

$$\boldsymbol{u}' = \boldsymbol{u} + R.C(i).\boldsymbol{x}$$

$$\begin{cases} C_u(i) \simeq 0.42\, i & \text{for an uniform brightness} \\ C_l(i) \simeq 0.7445 + 0.042\, i & \text{with Lambert's law} \end{cases}$$

These giving the lower and upper bounds of photocentre displacement.

We also find by least squares the parameters a and b of function $C(i) = a + b\,i$ that best fit the observations of a single minor planet. The problem of correlation still holds here so that

Table 2. Ephemerides improvement. Osculating elements were expressed in the ecliptic of J2000, for the epoch TE= 2 448 439.0 (jd). The variations of initial conditions are expressed in terms of a 6 parameters vector $\boldsymbol{dq} = (dl_o; dp; dq; dr; de; da/a)$. Values are in mas (the same transformation is applied on the dimensionless parameters de and da/a); standard deviation is given in brackets. See text for an explanation of the rank

No Name	Rank	$dr + dl_o$	dp	dq	$e\,dr$	de	da/a
3 -Juno	4	54.11	57.89	103.40	16.46	1.22	30.70
		(44.81)	(3.41)	(2.54)	(32.78)	(26.68)	(38.35)
5 -Astraea	4	406.88	-60.56	-156.49	352.32	472.40	598.71
		(99.88)	(5.56)	(2.20)	(39.08)	(68.50)	(106.51)
6 -Hebe	5	-38.80	15.82	39.16	-12.02	-56.74	-3.39
		(68.89)	(3.22)	(2.34)	(52.77)	(21.70)	(59.14)
18 -Melpomene	4	-130.97	59.02	172.55	68.19	42.46	6.87
		(143.31)	(6.76)	(4.62)	(55.34)	(89.25)	(99.20)
29 -Amphitrite	4	649.19	-82.20	-24.91	-39.59	232.24	-54.31
		(203.68)	(2.52)	(6.79)	(28.10)	(78.53)	(48.23)
39 -Laetitia	4	-107.70	73.83	73.04	-87.96	-0.41	116.76
		(59.82)	(2.42)	(1.84)	(41.31)	(26.08)	(51.45)
349 -Dembowska	4	-215.57	-10.37	134.61	-371.99	23.75	346.07
		(68.58)	(2.86)	(5.43)	(87.56)	(25.82)	(99.83)

only one parameter can be determined. We find the particular solutions:

Ceres: $a = 0.78 \pm 0.06$
Vesta: $a = 0.81 \pm 0.03$

When one is considering the photocentre displacement, Lambert's law is a good model of the light scattering on the surface of these minor planets. A persisting systematic trend for Vesta however is not accounted for by this model; this minor planet is known to have a dark spot.

5.4. Link of the kinematical and dynamical frames

So far the differences *observed minus computed position* have been investigated one minor planet at a time, by fitting new orbital elements. However the geocentric positions depend both on the heliocentric orbit of the minor planet and on the orbit of the earth, that is to say on the orbital elements and on the reference system used in the ephemerides compared to the Hipparcos sphere. The latter effect is common to all minor planets. The system to solve now is:

$$(o-c)_i = A_i \,.\, \boldsymbol{dq} + B_i \,.\, \boldsymbol{dq_i}$$

where $\boldsymbol{dq_i}$ is the correction to the elements of the ith minor planet. Vector $\boldsymbol{dq}$ contains the correction common to all observations $i.e.$ $\boldsymbol{dq_o}$, a linear combination of a correction to the earth ephemerides, and $\boldsymbol{W}$, the rotation of the Hipparcos sphere relative to the dynamical reference frame (DE 200). The system of equations can be written as:

$$\begin{cases} B_i \,.\, \boldsymbol{dq_i} = (o-c)_i \; - \; A_i \,.\, \boldsymbol{dq} \\ \sum_i (I_n - B_i.B_i^-) \,.\, A_i \,.\, \boldsymbol{dq} = (I_n - B_i.B_i^-) \,.\, (o-c)_i \end{cases}$$

Matrix $B_i^- = (B_i^t.B_i)^{-1}.B_i^t$, depends on the chosen parameters for $\boldsymbol{dq_i}$ only, so that there is no linear combination with $\boldsymbol{dq}$.

The corrections $\boldsymbol{dq}$ – smaller in magnitude than $\boldsymbol{dq_i}$– however depend on the photocentre displacement (Söderhjelm and Lindegren, 1982). They depend also on the solution retained for minor planets orbital correction: minimal rank dimension retained during the improvement of the orbital elements of a single minor planet. This sensitivity is shown on Table 3 for the Hipparcos sphere rotation only; no phase effect and no orbital correction for the Earth were considered here and 46 minor planets were used. This table gives the two sets of solution for the Hipparcos sphere rotation $\boldsymbol{W_0}$ and rotation rate $\boldsymbol{W_1}$. The total rotation expressed in the ecliptical frame J2000 is $\boldsymbol{W} = \boldsymbol{W_0} + (t - t_0)\boldsymbol{W_1}$ with t expressed in year from t_0 = 2 448 439.0 (jd). The solutions essentially differ for the component along the ecliptical pole; this can be explained by the fact that it reflects a constant rotation in the minor planets trajectory planes (they are close to the ecliptic). So a change on the strongly correlated parameters dr, dl_o, da/a and de due to the solution used propagates to the rotation in the ecliptical plane. At initial epoch, the plane of the ecliptic is tied with a precision of 1.1 mas and the equinox within 2.2 mas.

This particular value obtained for the sphere rotation ($\boldsymbol{dq_o} = \boldsymbol{0}$) is neither final nor can it be compared to the one obtained from the link of the Hipparcos star catalogue to the FK5. If we consider only the corrections in orientation for earth and asteroids ephemerides, keeping the same notation for the sake of brevity, we can write for the various rotations:

$$\boldsymbol{du} = \boldsymbol{u} \wedge \boldsymbol{W} - \boldsymbol{r} \wedge \boldsymbol{dq_i} + \boldsymbol{X} \wedge \boldsymbol{dq_o} \quad ; \quad \boldsymbol{u} = \boldsymbol{r} - \boldsymbol{X} - \boldsymbol{s}$$

with $\boldsymbol{X}$ and $\boldsymbol{r}$ being the earth and minor planet barycentric position, and $\boldsymbol{s}$ the satellite geocentric position. This latter vector can be neglected so that we have:

Table 3. Hipparcos sphere rotation. Values are in mas for the rotation and $mas/year$ for the rotation rate. The two sets are: least square solution (LS) and with Singular Value Decomposition (SVD)

	LS		SVD	
Rotation	W_0	rms	W_0	rms
W_{0x}	29.75	1.31	23.76	1.14
W_{0y}	-8.06	1.19	-19.16	1.11
W_{0z}	-90.55	3.07	-70.55	2.23
Rotation rate	W_1	rms	W_1	rms
W_{1x}	10.22	0.87	8.00	0.78
W_{1y}	-5.40	0.93	-2.72	0.82
W_{1z}	26.00	2.90	33.86	2.19

$$\boldsymbol{du} \simeq \boldsymbol{u} \wedge (\boldsymbol{W_o} - \boldsymbol{dq_o}) - \boldsymbol{r} \wedge (\boldsymbol{dq_i} - \boldsymbol{dq_o}) + (t - t_0)\, \boldsymbol{u} \wedge \boldsymbol{W_1}$$

When one is considering the complete set of global unknowns a quasi-indetermination persists. Actually the Hipparcos sphere orientation $\boldsymbol{W_o}$ cannot be determined here, only the rotation rate $\boldsymbol{W_1}$ – yielding a non rotating frame – is found explicitly. Note that a different approach for the same objective has been derived (Bec-Borsenberger et al., 1995). It is important that different methods be applied and compared.

At quadrature, a correction to the earth mean anomaly does not yield any change to the observed direction (Kovalevsky, 1982). Hipparcos observations of minor planets however occurs at elongation 43° on either side of the quadrature, thus earth and minor planets mean anomaly have to be determined. Following the work of B.V. Numerov (Numerov, 1935), we showed that the inclusion of less accurate ground-based observations made around oppositions yields a better separation of these quantities (Hestroffer, 1993). This can only be done once the Hipparcos sphere is tied to the FK5. Separability of the parameters associated to the sphere rotation ($\boldsymbol{W_o}$) and the earth's trajectory orientation at epoch ($\boldsymbol{dq_o}$) is more troublesome. Since DE200 system fixes the earth's orbit with greater accuracy (Williams et al., 1989), nothing is to be gained with classical ground-based observations (Branham et al., 1992) when the sphere orientation is considered.

On the other hand one can determine corrections to the FK5 equinox and equator by using ground based observations and Hipparcos observations linked to the FK5.

6. Conclusion

The 30-month data has been reduced showing the good quality of minor planets observations carried out by the satellite Hipparcos. The accuracy of the astrometric grid crossing normal points on the Hipparcos sphere is about 0.02 arcsec. Correction of the photocentre offset due to phase effect is well modelled when considering a spherical object and light scattering following Lambert's law; this offset is of importance when one determinine the Hipparcos sphere rotation rate. It has also been shown that the Hipparcos sphere orientation cannot be disentangled from the correction to the orbital elements of the earth, and only the difference between them can be solved for. However, the link of the kinematical and dynamical frames could be improved by adding ground based observations around opposition to the Hipparcos observations. Finally the rotation rate is determined with a precision of about two milli-arcsecond per year. The value obtained for the Hipparcos sphere rotation refers to the rotation between the frame defined in the minor planet ephemerides and the FAST 30-months solution; we should stress that this catalogue is not the same as the one discussed in Lindegren et al. (1995).

References

Balmino G. 1969, Méthode d'intégration de Bulirsh et Stoer, Ed. CNES.
Bec-Borsenberger, A., 1985, Proc. Aussois Coll. ESA SP-234, 175.
Bec-Borsenberger, A., 1989, ESA SP-1111, Vol 2, 213.
Bec-Borsenberger, A., 1992, A&A, 258, 94-98.
Bec-Borsenberger, A., 1993, A&AS, 98, 77-125.
Bec-Borsenberger, A., Bange, J.F. and Bougeard, M.L., 1995, A&A, this issue.
Branham, R.L. Jr and Sanguin, J.G., 1992, AJ, 103, 2099.
Brouwer, D., Clemence, L., 1961, Methods of Celestial Mechanics. Academic Press inc. London.
Bulirsh, R. and Stoer, J., 1966, Numerical treatment of ordinary differential equations by extrapolations methods, Num. Math., 8, 1-13.
Donati, F., Froeschlé, M., Falin, J.L., Canuto, E., Kovalevsky, J., 1992, A&A, 258, 41.
Ephemerides of minor planets for 1966, Institute of Theoretical Astronomy, Leningrad.
Hestroffer, D., 1993, in: 'Developments in Astrometry and their Impact on Astrophysics and Geodynamics', I.I. Mueller and B. Kolaczek (eds), IAU Symp. 156, 19.
Kovalevsky, J., 1982, Celest. Mech., 26, 213.
Kovalevsky, J., Falin, J.L., Pieplu, J.L. et al., 1992, A&A, 258, 7.
Kovalevsky, J., Lindegren, L., Froeschlé, M. et al., 1995, A&A, this issue.
Lindegren, L., 1977, A&A, 57, 55.
Lindegren, L., 1987, Third FAST Thinkshop , Bernacca P.L. and Kovalevsky J. eds, 285.
Lindegren, L. et al., 1995, present issue.
Morando, B., 1985, SecSecond FAST Thinkshop , Kovalevsky J. ed., 125.
Morando, B., 1987, Third FAST Thinkshop , Bernacca P.L. and Kovalevsky J. eds, 277.
Morando, B. and Lindegren, L., 1989, ESA SP-1111, Vol 3 , 269.
Numerov, B.V., 1936, Astron. J., 45, 105.
Söderhjelm, S. and Lindegren, L., 1982, A&A, 110, 156.
Standish, E.M. Jr, 1990 A&A, 233, 352.
Will, C.M., 1981, Theory and Experiment in Gravitational Physics.
Williams, J.G., Standish, E.M., 1989, in: 'Reference Frames', J. Kovalevsky, I.I. Mueller and B. Kolaczek (eds).

This article was processed by the author using Springer-Verlag TEX A&A macro package 1992.